

# Validation and Application of Jason-1 and Envisat Significant Wave Heights

Tom H. Durrant and Diana J. M. Greenslade  
CAWCR/Bureau of Meteorology  
Melbourne  
Australia

## Abstract

Satellite altimetry provides an immensely valuable source of operational  $H_s$  data. Currently, altimeters on-board Jason-1 and Envisat provide global  $H_s$  observations, available within 3-5 hours of real time. In this work,  $H_s$  data from these altimeters are validated against in situ buoy data from the National Data Buoy Center (NDBC) and Marine Environmental Data Service (MEDS) buoy networks. Data covers a period of three years for Envisat and over four years for Jason-1.

Co-location criteria of 50 km and 30 minutes yield 3452 and 2157 co-locations for Jason-1 and Envisat respectively. Jason-1 is found to be in no need of correction, performing well throughout the range of wave heights, although it is notably noisier than Envisat. An overall RMS difference between Jason-1 and buoy data of 0.229 m is found. Envisat has a tendency to overestimate low  $H_s$  and underestimate high  $H_s$ . A linear correction reduces the RMS difference by 8%, from 0.219 m to 0.202 m.

A systematic difference in the  $H_s$  being reported by MEDS and NDBC buoy networks is noted. Using the altimeter data as a common reference, it is estimated that MEDS buoys are underestimating  $H_s$  relative to NDBC buoys by about 10%.

The corrected altimeter data are used to make preliminary assessments of two potential upgrades to the Bureau of Meteorology's wave forecasting system – specifically, an increase in the directional resolution of the wave spectrum and the expansion of the data assimilation system to include Envisat  $H_s$  data as well as Jason-1. *In situ* buoy data are also used to assess the improvements in model forecast skill and the computational requirements of the potential upgrades are evaluated. It is concluded that in order to gain improvements in skill for both short-range and long-range (up to 72-hour) forecasts, then both of the proposed enhancements need to be incorporated.

## 1. Introduction

The Bureau of Meteorology (the Bureau) currently runs AUSWAM operationally, a version of the third-generation wave model WAM (WAMDI Group 1988). Forecasts of sea-state from AUSWAM are used as numerical forecast guidance for the Bureau's marine services. Details of the current implementation of AUSWAM can be found in (National Meteorological and Oceanographic Centre, 2002) and the references listed therein. Of particular relevance here is the directional resolution of the wave spectrum (currently set at 30°) and the data assimilation (DA) scheme, which includes Significant Wave Height ( $H_s$ ) data from the Jason-1 satellite altimeter only.

A directional resolution of 30° is relatively coarse, compared to other global operational wave forecasting systems, which are typically twice this. Coarse resolutions can save on

computational resources but there are potentially major negative impacts on the resulting wave forecasts. In particular, a coarse directional resolution constrains the wave energy to propagate in a limited number of directions. This can lead to undesirable features as, for example, swell propagates long distances across the ocean surface and results in "clumping" of the wave energy. This is called the "sprinkler effect". There are various techniques that can be used to minimize the sprinkler effect – e.g. increasing the angular resolution of the wave spectrum by including more directional bins, adding diffusion to the propagation terms etc. (Tolman, 2002a). Future plans within the Bureau's operational systems involve potentially replacing the current wave model, so for time being, we consider the simplest method, which is to increase the angular resolution.

The Bureau currently receives  $H_s$  data in real-

time from the Envisat satellite altimeter, in addition to the Jason-1 observations, so there is also the opportunity to expand the DA system by including this additional source of data. One of the main limitations of assimilating satellite altimeter data is the sparseness of the data, so including observations from two satellites with different orbit characteristics, and thus different sampling patterns, could be expected to improve the skill of the wave forecasts.

Traditionally, *in situ* buoy data are used to verify potential upgrades to the wave modelling system, such as those described above. The root-mean-square (RMS) difference between model forecast and buoy  $H_s$  is typically used as a “skill score” and if this can be reduced, this is seen as a positive gain for the wave model system and the change is duly implemented (e.g. Greenslade and Young, 2004). The advantage of using buoy observations to verify the model forecasts is that they are not used in the DA system and so they represent a completely independent data source.

However, the use of buoy data alone for model verification does have its limitations. Buoy data typically are only available near the coast, so while modelled  $H_s$  may be improved at those particular areas, it may not be true everywhere in the domain. It could be argued that wave model skill in the high seas regions is just as relevant for the Bureau’s Marine Services than skill at the coast, so this is a particular deficiency of using *in situ* buoy data to verify model changes.

A new technique for verifying the wave model is developed here and this is via the use of satellite altimeter data over the open ocean. The global coverage makes these observations ideal for model evaluation and the diagnosis of potential model errors. The Fast-Delivery (FD) altimeter products examined here (discussed further in section 3.1) are received at the Bureau within three hours of observation. Previous work has shown that FD data typically contain systematic errors (e.g. Cotton and Carter, 1994), although the precise nature of these errors has also been found to vary

somewhat from mission to mission. Careful calibration of these data is thus required before they can be used with confidence.

In this work, FD  $H_s$  from both the Jason-1 and Envisat altimeters is validated against *in situ* buoy data. A number of correction schemes are then investigated with the aim of minimising the overall RMS difference. Section 2 summarises the previous validation work for each altimeter. Section 3 examines the data and method used, followed by a discussion of the results in Section 4. In Section 5 these results are applied to the altimeter data streams and these are then used to assess the potential upgrades to the wave forecasting system discussed above. Finally Section 6 provides a summary.

## 2. Previous Validation Studies

Seven satellite altimeters have been deployed since 1985, providing the first long term global observation of sea level, wind speed and wave height. Steady improvement has been made with each subsequent satellite, however, characteristic biases have tended to vary somewhat from one to the next. Careful calibration of altimeter estimates against *in situ* measurements is thus important for accurate global estimation of  $H_s$ .

Altimeter validation studies in general attempt to obtain a set of co-located altimeter and buoy observations and find an appropriate adjustment for the altimeter which results in the best fit with the *in situ* buoy data. Comparisons between buoy and altimeter derived  $H_s$  data are complicated by the fact that each is measuring different aspects of the temporally and spatially varying wave field (Monaldo, 1988), and hence may differ, even in the case that both instruments are making perfectly accurate estimates. These differences can be divided into three categories, temporal proximity, spatial proximity and sampling variability associated with time and space averaging. Due to the frequency of satellite passes, altimeter-buoy measurements can not always be made simultaneously. Usually, a temporal window of

acceptability is established; a maximum time difference for measurements to be considered a comparable altimeter-buoy pair. Similarly, an acceptable spatial separation between the altimeter track and the buoy location must be established. Sampling variability occurs due to the fact that altimeter measurements are essentially an instantaneous spatial average of  $H_s$  over the altimeter footprint area, which increases from a diameter of about 3 km for small wave conditions to about 10 km for large wave conditions, while buoy measurements are time-averaged measurements of  $H_s$  at a point location.

Based on assessments of the spatial and temporal variation of the wave field, Monaldo (1988) proposes co-location criteria of observations occurring within 50 km and 30 minutes of one another. These criteria have been widely adopted since, and now provide the standard for this type of work.

The two altimeters examined in this work are on-board the currently flying Jason-1 and Envisat satellites. Launched in December 2001, Jason-1 is a jointly operated project between the French and U.S. space agencies, the CNES and the NASA respectively. It follows on from the enormously successful TOPEX mission, sharing the same orbital parameters and following in the same ground tracks as its predecessor. It flies in a non-sun-synchronous orbit at an altitude of 1336 km and an inclination angle of 66°. It carries a Poseiden-2 altimeter, derived from the experimental Poseiden-1 instrument carried on the TOPEX mission. Detailed descriptions of the mission and the Poseiden-2 altimeter can be found in Ménard et al. (2003) and Carayon et al. (2003) respectively. Envisat, launched March 2002, is operated by the ESA. This mission follows on from ERS-1 and ERS-2, carrying the so-called RA-2 altimeter derived from these earlier missions. Envisat flies in a sun-synchronous orbit at an altitude of 800 km. In contrast to the pro-grade orbit of Jason-1, Envisat has a retrograde orbit of 98° allowing measurement closer to the poles. More detail can be found in

Resti et al. (1999).

Multiple data streams are available from these satellites. These can be divided into operational, or so called FD streams, and higher accuracy, more detailed off-line streams. The former is used primarily for operational DA and is available within 2-3 hours of observation, while the latter is typically available several days later. Radar altimeters are active microwave sensors which infer  $H_s$  directly from the shape of the radar pulse, or waveform, returning to the nadir looking altimeter. FD products differ primarily from their off-line counterparts by the fact that the former consists of reports derived from on board processing of these waveforms, while ground based processing is performed for the off-line stream. In this work, it is the FD stream we wish to validate. These are referred to as the OSDR in the case of Jason-1, and the NRT stream for Envisat.

Although both Jason-1 and Envisat have been in orbit for a number of years, there is little published work on the validation of  $H_s$  data from these satellites, especially the FD products. The following summarises the published validation studies for each altimeter.

## 2.1. Jason-1

Though there is little validation work available for FD Jason-1 data, there has been some work examining the off-line product. Before these studies can be used as a context for the work presented here, we must know how the FD and off-line products compare. Desai and Vincent (2003) investigated precisely this, comparing 40 days of data from each stream. Inclusion of sea state bias calculations based on (among other things) wind and wave conditions in the off-line product result in significant differences between these streams for sea surface height data. However, for  $H_s$ , they conclude that while the FD product does show slightly less scatter, only small systematic differences exist between the FD and off-line products, which appear to be well described by the linear relationship:

$$H_s^{OL} = 1.053 H_s^{FD} + 0.011m \quad (1)$$

Assuming the validity of this result, we now consider some work validating off-line  $H_s$  data with in situ buoy data. One of the earliest studies was performed by Ray and Beckley (2003) using 6 months of off-line data from February to August 2002. They find a 7 cm negative bias, suggesting a correction of:

$$H_s^{adj} = 1.100H_s^{OL} - 0.0104m \quad (2)$$

However, this study may be of limited reliability, with conclusions made based on only 368 co-locations.

In an attempt to provide a homogeneous data set spanning several satellites, Queffeulou (2004) validates  $H_s$  data from six altimeters, using cross-altimeter and buoy comparisons. Using 50 km along track averages and a co-location separation criteria of 30 minutes his study covers the period January 2002 to September 2003 and resulted in 2853 co-locations for Jason-1. Overall, he found a 5 cm negative bias in the altimeter data relative to the buoy data, recommending corrections of:

$$H_s^{adj} = 1.0072H_s^{OL} + 0.0392m \quad (3)$$

Substituting equation 1 into equations 3 and 2 gives the following corrections to FD data:

$$H_s^{adj} = 1.0605H_s^{FD} + 0.0503m \quad (4)$$

$$H_s^{adj} = 1.158H_s^{FD} + 0.002m \quad (5)$$

respectively.

Research at Meteo-France (Lefevre, personal communication, 2006) has shown biases to be small, and FD data is not corrected prior to assimilation. ECMWF applies a correction of (Bidlot, personal communication, 2006):

$$H_s^{adj} = 0.9615H_s^{FD} - 0.0104m \quad (6)$$

This reduction of about 4% is based on comparisons with buoy and model data.

## 2.2. Envisat

Abdalla (2006) has carried out a thorough investigation on Envisat FD wind-wave performance based on data from July 2002 to October 2003. Although no correction is proposed, they estimate that the altimeter overestimates  $H_s$  by about 9 cm relative to buoy data.

Queffeulou (2004) performed a validation of Envisat  $H_s$  data, using 30 minute temporal and 50 km spatial windows, from April 2003 to February 2004, yielding 1280 co-locations. He proposes a correction of:

$$H_s^{adj} = 1.0327H_s^{OL} - 0.1830 \quad (7)$$

This is however, using the off-line product, and while the results of Desai and Vincent (2003) mentioned above regarding comparisons between FD and off-line data for Jason-1 are encouraging, the relationship between these two streams for Envisat remains unknown.

ECMWF applies the same correction to Envisat as is applied to the Jason-1 data, i.e. a bulk reduction of 4% (Bidlot, personal communication, 2006)

## 3. Altimeter Validation Method

### 3.1. Data

Buoy data are generally assumed to be of high quality, and have been used in numerous studies for validation of model (eg Janssen et al., 1997; Caires and Sterl, 2003; Caires et al., 2004) and altimeter (eg Tolman, 2002b; Queffeulou, 2004; Faugere et al., 2006) data. Buoy data used in this work are obtained from two buoy networks, the U. S. operated NDBC network and the MEDS network operated by Environment Canada. Buoy data from the Australian network were considered, however, buoy locations were too close to the coast, or reporting frequency too low to be of use in this study. In the case of both selected networks, rigorous quality control is undertaken by these institutions, with bad data being either flagged, or removed completely from the data set. These

networks are a dynamic set of buoys, with new buoys regularly being added, and others being removed.

Altimeter data was obtained from several sources. Envisat data was extracted from the Bureau archive for the period from September 2004 through to April 2006, with earlier data from April 2003 being obtained from CNES. Similarly, Jason-1 data was extracted from the Bureau archive for the period from September 2004 through to the end of March 2006 with data from January 2002 obtained from Meteo-France. For each altimeter, a month of overlapping data was analysed to ensure consistency from the two sources, and accurate decoding. This gave data sets covering a period of three years for Envisat, and four and a half for Jason-1.

### 3.2. Method

Though a 50 km spatial proximity criterion, or thereabouts, is widely used for altimeter validation studies, it is often replaced by a latitude longitude proximity in order to ease calculation (e.g. Janssen et al, 1997; Caires and Sterl, 2003; Greenslade and Young, 2004.) This was the initial approach taken here. However, it became apparent that differing error characteristics arose for each altimeter by virtue of this technique due to the different orbital characteristics of their respective orbits. Hence, a strict 50 km great arc circle proximity requirement was adopted. A more complete discussion of the use of latitude longitude proximity and an assessment of its weaknesses can be found in Durrant et al (submitted).

At each buoy, consecutive altimeter observations crossing an area within a 50 km radius of the buoy location were grouped together. Passes took less than a minute to traverse this area, with each pass typically resulting in 15-18 individual observations that can be assumed to be simultaneous. These data were quality controlled by removing individual

observations greater than two standard deviations away from the mean for that pass. Hourly buoy data were then linearly interpolated to the altimeter overpass time, with the additional criterion that there be at least one buoy observation within one hour before and one hour after the time of the altimeter overpass. This interpolated buoy data and the mean of the quality controlled altimeter observations made up a single co-location. To eliminate interference from land, buoys were required to be greater than 50 km offshore. The resulting set of buoys included in this analysis is shown in Figure 1.

Two different correction schemes are presented here, a simple bias correction, and a linear model. Two-branched linear functions were also investigated, whereby co-located data are divided into two segments, above and below a particular altimeter  $H_s$  ‘cut-off’ value, and a linear correction then applied separately to the two segments of data. A number of different cut-off values were investigated, however, these functions provided no better results than the simple linear model.

During the early altimeter missions, errors associated with buoy data were small relative to those of the altimeter. As such, buoy data were generally regarded as ‘truth’ and hence the correct procedure was to regress the altimeter data onto the buoy data, i.e., perform a regression with the altimeter data as the independent variable and the buoy data as the dependent variable. However, it is now accepted that buoy and altimeter data have comparable error variances (Caires and Sterl, 2003) and regression techniques must account for errors in both data sets. An appropriate alternative method, and that adopted here, is to perform two regressions, one with the buoy data as the independent variable and one with the altimeter data as the independent variable

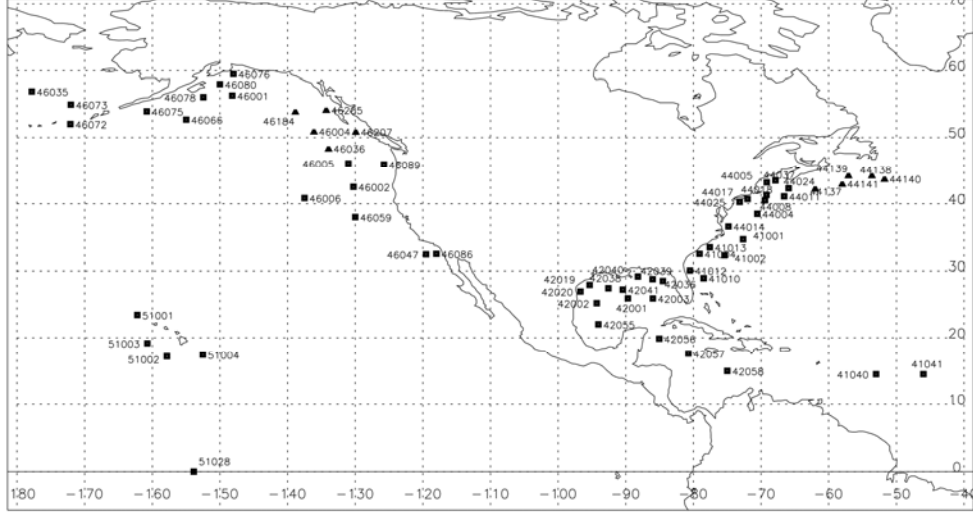


**Figure 1** Buoys used in this study. Buoys from the NDBC are marked with squares and those from the MEDS network are marked with triangles

and then take the average of the two regression lines as the final result (Bauer and Staabs, 1998). This method assumes equal error variance in the altimeter and buoy  $H_s$  measurements.

The statistics used here are the bias, RMS difference, Scatter Index (SI) and correlation coefficient (R), defined as follows:

$$Bias = \frac{1}{N} \sum_{i=1}^N A_i - B_i \quad (8)$$

$$RMS = \sqrt{\frac{1}{N} \sum_{i=1}^N (A_i - B_i)^2} \quad (9)$$

$$SI = \frac{\sqrt{\frac{1}{N} \sum_{i=1}^N ((A_i - \bar{A}) - (B_i - \bar{B}))^2}}{\bar{B}} \quad (10)$$

$$R = \frac{\sum_{i=1}^N (A_i - \bar{A})(B_i - \bar{B})}{\sqrt{\sum_{i=1}^N (A_i - \bar{A})^2 (B_i - \bar{B})^2}} \quad (11)$$

Where  $A_i$  is the altimeter  $H_s$ ,  $B_i$  is buoy  $H_s$ ,  $N$  is the number of co-locations and an overbar represents the mean value.

#### 4. Validation Results

##### 4.1. MEDS and NDBC buoy network differences

This analysis revealed an apparent systematic difference between  $H_s$  estimates from the MEDS and NDBC buoy networks. Figure 2 shows scatter plots of co-locations for both altimeters for both NDBC and MEDS buoys separately. In the case of both satellites, it is clear that the MEDS buoys are underestimating buoy  $H_s$  measurements relative to the altimeter. Jason-1 shows little bias relative to NDBC buoys, but a 27 cm bias relative to the MEDS buoys. Similarly for Envisat a small bias of 4 cm relative to NDBC buoys compares to 28 cm for the MEDS co-locations. This systematic underestimation appears to be linearly related to  $H_s$ . The SI indicates a similar amount of noise for comparisons with both altimeters, suggesting a comparable level of noise for the buoy networks relative to each other.

These differences have been noted in several previous studies. Most recently, in examining TOPEX, Jason-1 and ENVISAT wave heights, Queffeulou (2006) showed that the validation

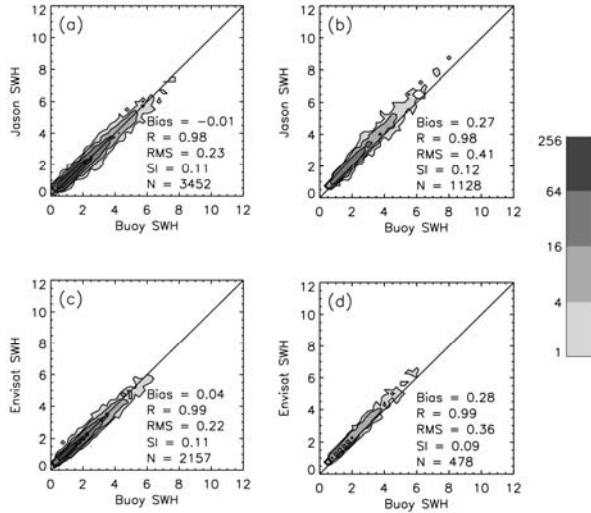


**Figure 2** Scatter plots of co-located  $H_s$  observations for Jason-1 and Envisat for both the NDBC (left hand panels) and MEDS (right hand panels) buoy networks separately with the number of co-locations in each 0.5 m bin contoured

results are different according to the buoy network, and in the same way for the 3 altimeters. For instance, the TOPEX - buoy mean bias is -0.01 m for the NDBC network and 0.19 m for the MEDS network, with similar results reported for the other satellites. Examining two years of altimeter data, Cotton et al. (2004) also identify significant differences in validation results for Envisat and ERS-2 in reference to different buoy networks, with results again showing a greater altimeter bias when compared to MEDS buoys than for that of NDBC buoys. Similar results are also noted in the work of Challenor and Cotton (2001). They present altimeter verification results for all altimeters since Geosat against several buoy networks. They show that the Japanese buoys measured  $H_s$  highest (+6% cf NDBC), then the UK buoy network (+4%), then NDBC (as the reference), with the Canadian network buoys measuring the lowest (-5%). However, it is noted that the errors in these analyses were quite high, because at the time, the  $H_s$  data supplied by the UK Met Office and Japan Meteorological Agency were only provided to the nearest 0.5 m. The size of the buoy platform was investigated as a possible cause of the

discrepancy but no significant dependency was identified. They conclude that the differences are likely largely due to different reporting standards and quality control.

To quantify the difference between buoy networks, altimeter  $H_s$  estimates were taken as a reference for which each buoy network could be compared. Reference to the altimeter  $H_s$  as truth is deliberately avoided here. As discussed in section 3.2 neither buoy nor altimeter measurements can be regarded as truth and both must be assumed to contain errors. However, under the assumption that the altimeter provides self-consistent, and repeatable measurements, it is valid to employ it as a common reference.

For each network, a regression is performed with buoy data as the independent variable and the altimeter data as the dependent variable. This provides altimeter  $H_s$  as a linear function of both NDBC and MEDS buoys, given by equations 12 and 13 respectively for Jason-1 and 14 and 15 for Envisat.

$$H_s^{JAS} = 0.947 H_s^{NDBC} - 0.099m \quad (12)$$

$$H_s^{JAS} = 1.050 H_s^{MEDS} - 0.143m \quad (13)$$

$$H_s^{ENV} = 0.909 H_s^{NDBC} - 0.222m \quad (14)$$

$$H_s^{ENV} = 1.023 H_s^{MEDS} - 0.225m \quad (15)$$

These expressions are then equated to give a relationship between the two buoy networks. This yields the following linear relationships between MEDS and NDBC buoy  $H_s$  estimates as determined from Jason-1 (16) and Envisat (17) as a reference:

$$H_s^{MEDS} \approx 0.90 H_s^{NDBC} - 0.054m \quad (16)$$

$$H_s^{MEDS} \approx 0.889 H_s^{NDBC} - 0.003m \quad (17)$$

This suggests that MEDS buoys are underestimating  $H_s$  relative to NDBC buoys by about 10%. The source of this discrepancy remains unclear, though work is currently underway to investigate this further (Bidlot

et al., in prep). Initial investigations carried out in the present study suggest that it is not environmental. Examining each buoy individually reveals consistent biases amongst buoys in the same network, regardless of their geographical location. Buoy size is also unlikely to be the cause. Again, the consistency within each network, despite each being made up of buoys of various makes and sizes, suggest this is not a significant contributor. Though no evidence is presented here, the authors are inclined to agree with the conclusions of Challenor and Cotton (2001), that reporting standards and quality control are likely the primary cause. The magnitude of these differences highlights the need for increased calibration and communication of processes and practices among the international wave measurement community.

For the purposes of the altimeter validation, in order to ensure a consistent reference data set, only NDBC buoys are used, with all MEDS data removed from the analysis. This choice was motivated by the fact that the NDBC data set is much larger than the MEDS data set. NDBC data has also been more extensively used for this type of work, thereby providing the logical choice in the interests of providing a consistent data set across several satellites.

## 4.2. Results

Using only NDBC buoys yielded 3452 co-locations for Jason-1, and 2157 for Envisat. These co-located data points are shown in Figure 3. The following section assesses the performance of each altimeter, and examines various different functions to find a best fit to these data in order to devise a correction scheme.

Table 1 shows the validation statistics for the raw Jason-1 data set and those for the bias corrected and linearly corrected data sets. The uncorrected data shows a negative bias of only 1 cm and an RMS of 23 cm. Neither correction results in improvements to the RMS error, suggesting that Jason-1 requires no correction.

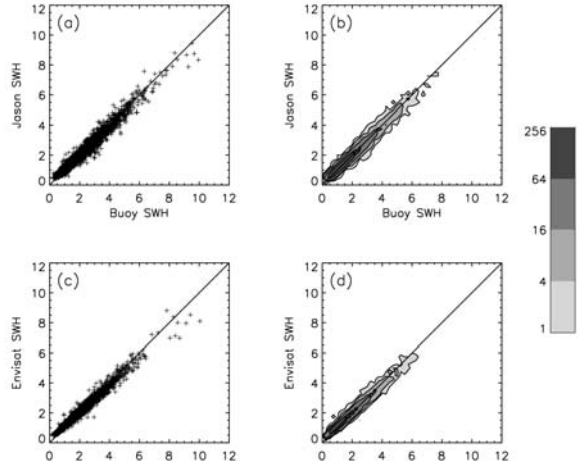


**Figure 3** (a) Co-located Jason-1 and buoy data and (b) the same data with the number of co-locations in each 0.5 m bin contoured. (c) and (d) show the same for Envisat data

**Table 1** Validation statistics for raw, bias corrected and linearly corrected Jason-1 data based on NDBC buoy comparisons

	Bias (m)	SI	RMS (m)	R
No adjustment	-0.010	0.110	0.229	0.983
Bias correction	-0.000	0.110	0.229	0.983
Linear correction	-0.000	0.110	0.229	0.983

As mentioned in Section 2.1 Ray and Beckley (2003) and Queffeulou (2004) found small negative biases, while the findings of Abdalla (2006) suggest a small positive bias. Overall, all these studies propose minor corrections, and are consistent with the findings of this work. These perspectives are also in line with those of Meteo-France, who currently don't apply a correction to Jason-1 fast delivery data prior to assimilation.

Table 2 shows the same validation statistics for Envisat. There is a small overall bias of 3.6 cm, with the altimeter overestimating  $H_s$ .

**Table 2** Validation statistics for raw, bias corrected and linearly corrected Envisat data based on NDBC buoy comparisons

	Bias (m)	SI	RMS (m)	R
No adjustment	0.036	0.106	0.219	0.986
Bias correction	0.000	0.106	0.216	0.986
Linear correction	0.000	0.099	0.202	0.986

Examining Figure 3 more closely, it appears that Envisat is overestimating low  $H_s$  and underestimating high  $H_s$ . As a result of this, applying a straight bias correction does little to improve the RMS error. Once again, it appears that a linear correction is the most suitable, producing more improvement than seen for Jason-1. The proposed correction is given by:

$$H_s^{adj} = 1.085H_s^{FD} - 0.213m \quad (18)$$

This correction results in a decrease in Envisat  $H_s$  for waves below 2.49 m and an increase above. Overall, RMS is reduced by 8%, and the SI by 7%.

#### 4.3. Discussion and Comparison

In terms of the need for bias corrections, Jason-1 seems to out-perform Envisat. However, Jason-1 is the noisier of the two, with the RMS difference being slightly higher than Envisat, despite its biases. Once Envisat is corrected, its RMS is 0.201 m compared to 0.229 m for Jason-1. This relative noise between the two altimeters has also been noted by Abdalla et al. (2005).

An increased level of noise has been noted for Jason-1 compared with its predecessor TOPEX (Ray and Beckley, 2003; Cotton et al., 2001; Quefféulou, 2006). Envisat on the other hand, appears to have shown significant improvements over its predecessor ERS-2, which suffered from systematic errors at low  $H_s$  (Greenslade and Young, 2004). However, it is

worth noting that, once a branched linear correction was applied, the RMS error reported by Greenslade and Young (2004) for ERS-2 was similar to that found here for the Envisat corrected data. This suggests that while the systematic biases are still being reduced with each altimeter mission, random error, or noise is levelling out. This also suggests that a large proportion of the RMS error seen in these results is from the sampling issues discussed in section 2. The previously mentioned work of Monaldo (1988), upon which much of the validity of studies of this nature are predicated, states an expected buoy altimeter RMS error of 0.4 m assuming perfect measurements from both instruments, due to these sampling issues alone. The fact that we are now seeing results that are better than these theoretical limits suggests that that estimate is in need of revision.

The apparent difference between the variance for each altimeter suggests that the assumption of equal error variances between buoy and altimeter is perhaps a generous one. As the regression technique used here relies on this assumption, the analysis would benefit from a more general approach such as that taken by Soukissian and Kechris (2007) which allows for differing error characteristics in the respective variables. However, as the corrections found here are small, this is unlikely to have a significant impact on results.

#### 5. Model Verification

Given the altimeter validation results found in the previous section, we can now be confident that the errors in the altimeter data are small and they can be used to verify some potential changes to AUSWAM, the Bureau's operational wave model. Specifically, the changes that are evaluated here are a) a doubling of the directional resolution of the wave model spectrum and b) the incorporation of Envisat  $H_s$  data as well as Jason-1 in the DA system. Both of these potential upgrades will require substantial increases in computational requirements, so the potential improvements in forecast skill that they provide are also

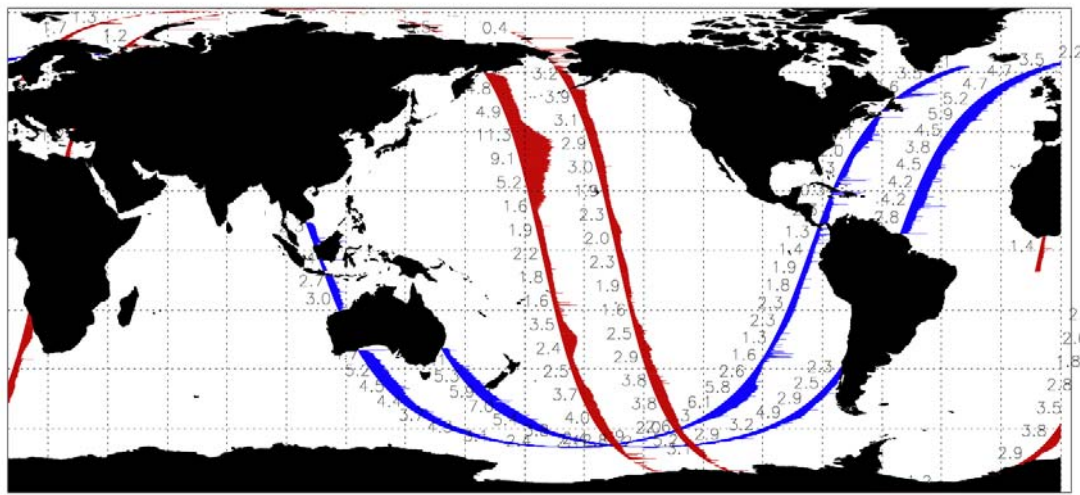


**Figure 4**  $H_s$  observations (m) from Jason-1 (blue) and Envisat (red) in a 3-hour time period centred on January 15, 0900Z.

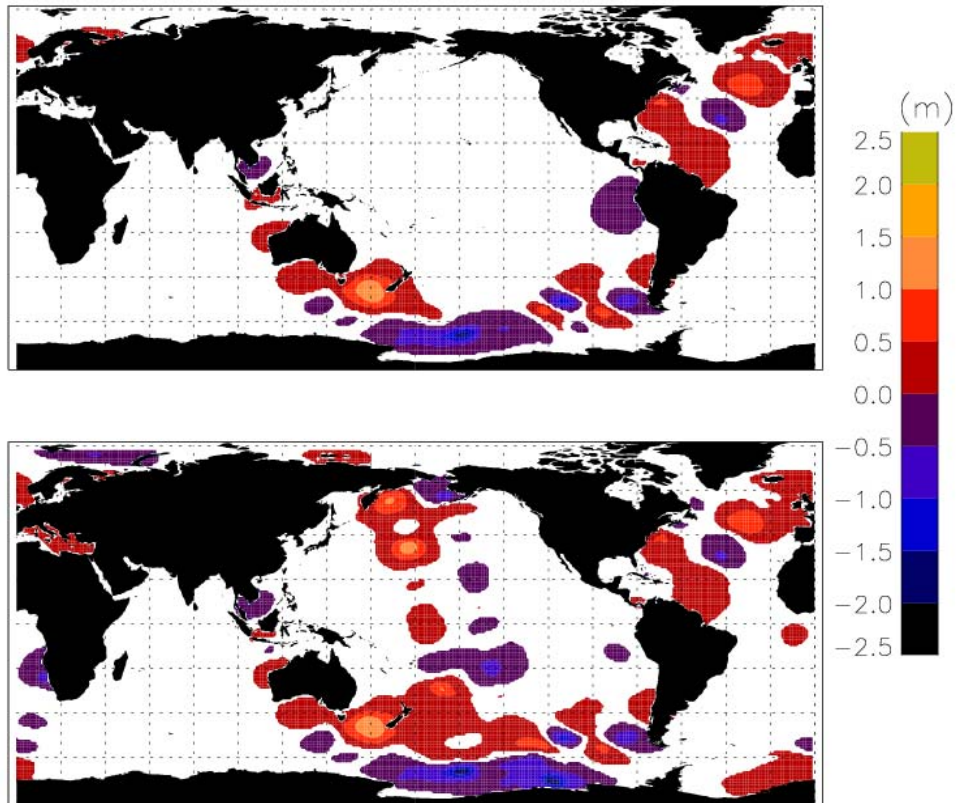


**Figure 5** Increment fields of  $H_s$  for the case of Jason-1 data alone (top panel) and both Jason-1 and Envisat (bottom panel) for the data shown in Figure 4, i.e., the assimilation period January 15, 0900Z.

considered in the context of the relative increase in computational requirements that they impose.

Several model runs were performed over the month of January 2005. All model runs were on the global domain ( $0\text{--}360^\circ$ ,  $78^\circ\text{S}$  –  $78^\circ\text{N}$ ) at  $1^\circ$  spatial resolution. All runs used the same wind forcing fields from the Bureau's global atmospheric model. 72-hour forecasts were made every 12 hours, after a 12-hour hindcast period, during which DA was performed (for the DA runs). DA was performed as in the current operational system (Greenslade and Young, 2005). Throughout this section, the altimeter data are corrected according to Section 4.2, specifically, a small linear correction described by equation 18 was applied to Envisat data, and no correction was applied to Jason-1. The model runs were as follows:

**Noassim-12:**

- 12 directional bins
- No assimilation

**Noassim-24:**

- 24 directional bins
- No assimilation

**Jason-12:**

- 12 directional bins
- Assimilation with Jason-1 data only

**Jason-24:**

- 24 directional bins
- Assimilation with Jason-1 data only

**Both-12:**

- 12 directional bins
- Jason-1 and Envisat data assimilated

**Both-24:**

- 24 directional bins
- Jason-1 and Envisat data assimilated

The current Bureau operational configuration is Jason-12.

Figure 4 shows the data coverage from the two satellites in a typical 3-hour DA period and Figure 5 shows a comparison of the resulting increment fields for the case of assimilating Jason-1 alone, and assimilating both satellites. It can be seen that a considerably larger portion

of the global wave field is updated when both satellites are assimilated, so this would be expected to have some impact on the forecasts.

It is also interesting to examine how these increments vary with time. We know that the modelled winds are typically underestimated (Schulz *et al.*, 2007) and that the  $H_s$  is also underestimated (Greenslade *et al.*, 2005) because of this, so we would expect that the initial modelled wave fields, on January 1<sup>st</sup> after the one month spin-up period have a significant amount of negative bias. The DA scheme, starting on January 1<sup>st</sup> would act to eliminate some of this bias, and since the changes to the wave field brought about by the DA take some days to decay (Greenslade and Young, 2005), then over the month, the magnitude of the increments should decrease. Figure 6 shows a time series of the mean absolute value of the increment for the Both-12 and Both-24 model runs. (This mean value does not include grid-points where the increment is equal to zero, in order to eliminate the effect of varying amounts of altimeter data for each assimilation period). We see that this is indeed the case: for the first few assimilation periods, the magnitude of the increment is relatively large, then over the first week, the increments become smaller and for the remainder of the month, they oscillate around a value of approximately 0.13m.

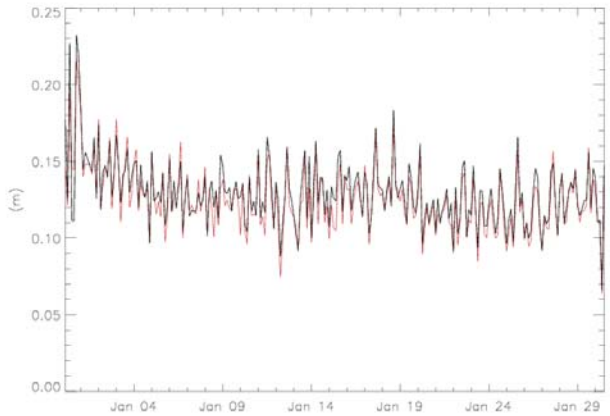


**Figure 6** Time series of the mean absolute value of the increment field for Both-12 (black) and Both-24 (red) model runs.



**Figure 7** Locations and names of the buoys used for verification of the model runs.

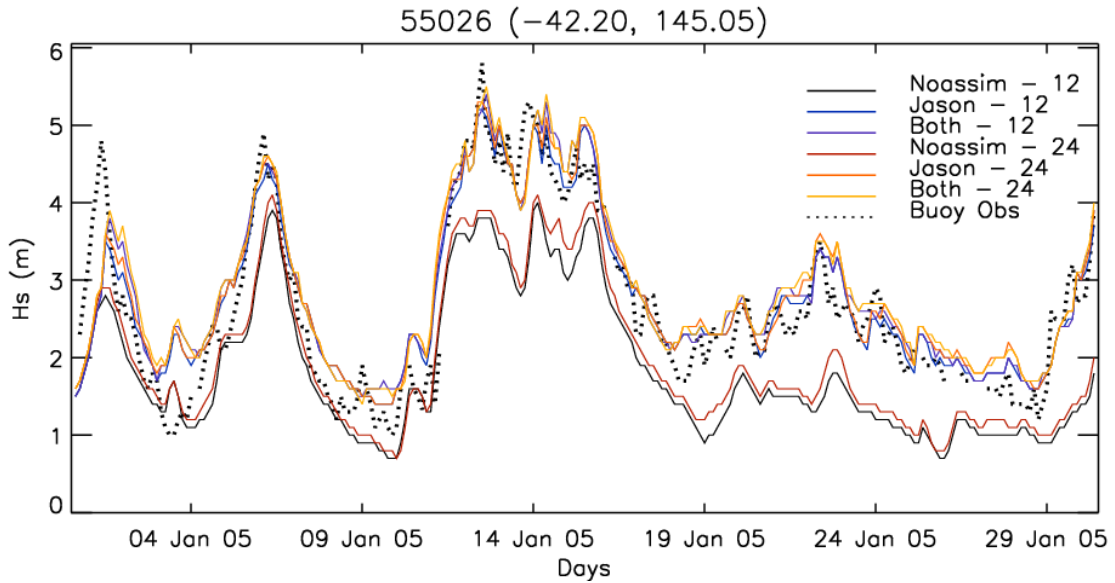


**Figure 8** Time series of  $H_s$  at buoy 55026 and the modelled 24-hour forecasts.

Figure 6 also shows a comparison of the increments between the runs with different directional resolution, but the same amount of altimeter data. One expected result of increasing the directional resolution is that the model should distribute the wave energy more accurately over the model grid, and so the corrections needed from the DA should be lower. It is not obvious from the figure, but an examination of the magnitude of the increments

shows that the mean value is indeed lower for the model run with 24 directional bins in about 75% of the DA periods.

The skill of each model run is evaluated here by comparison with observations – firstly with *in situ* buoy data in the Australian region and secondly, some preliminary evaluations against global altimeter observations are performed.

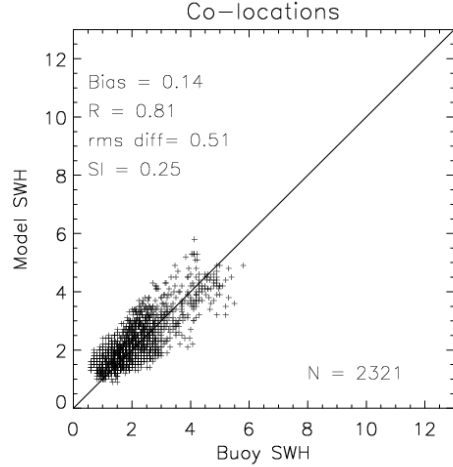
## 5.1. Evaluation against buoy data

The locations of the buoys used for verification of the model runs in this work are shown in Figure 7. Only buoys in the Australian region located in water deeper than 40 m are used here. Observations of  $H_s$  are available from some of the buoys at half-hourly intervals (55040, 55026 and 55035), some of the buoys at hourly intervals (55018, 55019, 55022, 55014, 55020) and the remainder at 3-hourly intervals.

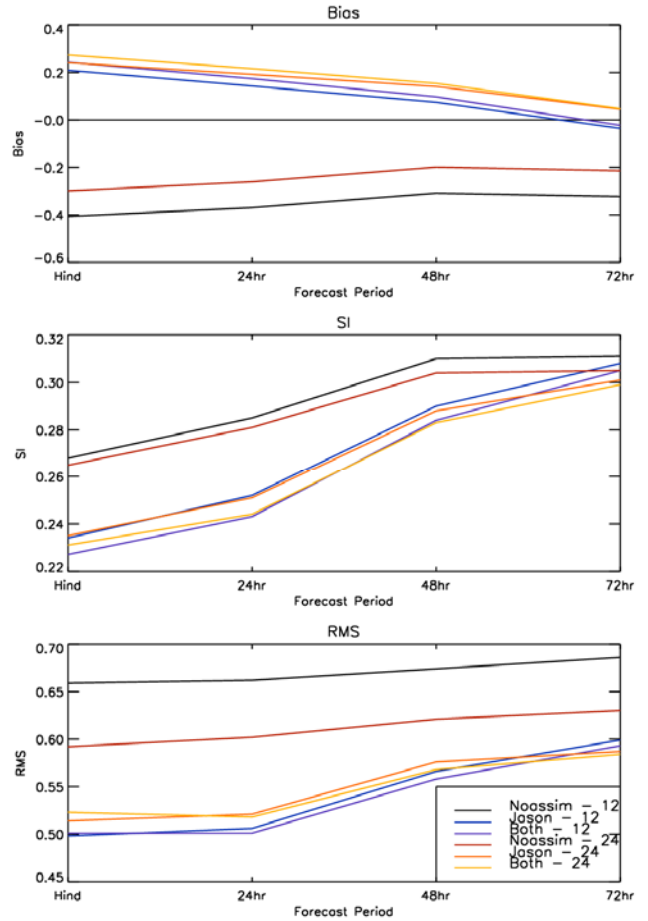
Linear interpolation in time was used to compare the time series of  $H_s$  from each buoy to the 3-hourly time series of  $H_s$  at the closest model gridpoint from each run.

Figure 8 shows the time series of 24-hour forecasts at buoy 55026. The underestimation of  $H_s$  from the model runs without DA can clearly be seen here and the DA significantly improves the overall model bias at this location. Note that the increase in the directional resolution of the wave spectrum has also reduced the bias slightly. The verification statistics described in equations 8 to 11 are calculated here for all model runs and 4 different forecast periods: hindcast, 24-hour, 48-hour and 72-hour forecasts. Note that the model output is archived every 12 hours at 3-hourly intervals, so the 24-hour forecast, for example, will actually consist of a recurring series of 15-, 18-, 21- and 24-hour forecasts. Here, the model-buoy co-locations for all buoys are treated as one individual dataset and statistics are calculated overall. For example, Figure 9 shows the co-located buoy and model  $H_s$  for all buoys for the Jason -12 model run.

The verification statistics are also shown in this figure and demonstrate that overall, this model run has a small (14 cm) positive bias relative to the buoys and an RMS difference of 51 cm. Overall statistics for all model runs are shown in Figure 10.



**Figure 9** Co-located buoy and model  $H_s$  for the Jason-12 model run for all 12 buoys.



**Figure 10** Summary of verification statistics (Bias, Scatter Index and RMS difference) for all model runs compared to the buoys shown in Figure 7.

There are several points of interest in these summary statistics. Firstly, it can be seen that overall, the bias for the DA cases is positive – particularly for the hindcast and short forecast ranges. Upon inspection of the statistics for individual buoys, it was found that these high positive bias values are dominated by buoys 56004 and 56005 on the West Australian coastline. These are in the shallowest water (between 40 and 50m) so the overestimation of  $H_s$  at these locations could be due to shallow water effects, i.e., the observed  $H_s$  may be reduced at these locations due to bottom friction, but the model doesn't capture this as it does not incorporate shallow water physics. It should be noted, however, that this positive bias does occur (but to a much lesser extent) at almost all buoy locations, so shallow water effects are unlikely to be a major contributor. An alternative explanation could be that the positive bias is an artifact of simply choosing the closest model gridpoint in a relatively coarse ( $1^\circ$ ) grid, as opposed to interpolating the model fields. This would result in a positive bias because the model gridpoint is always further offshore than the buoy location, and  $H_s$  typically increases with distance from the coast. Alternatively, it could be actual effect – the DA is perhaps over-compensating somehow for the negative bias in the non-assimilated fields. This will be discussed further in the next section, where the model runs are compared to the altimeter data.

Another point to note from these results is that, as seen in the case of buoy 55026, the increase in the directional resolution has reduced the model's negative bias considerably. It has also reduced the variable errors in the run with no DA, as seen in the SI, so this suggests that it is an improvement overall.

However, it appears from the SI results that if the directional resolution of the current model implementation is increased (i.e. Jason-12 to Jason-24), then the variable errors are only improved for the longer forecast ranges. This is also true for the case of assimilating both satellite data streams – in fact, in this case, the

lowest variable errors are from the model run with the coarser directional resolution. A possible explanation for this is that the directional increase has only a small impact, but it is effective for all forecast periods. For the short range forecasts, the DA improvement dominates the verification statistics, so it is only for the longer range forecasts, when the impact of the DA has decayed that gains are made by increasing the directional resolution.

The RMS values here are dominated by the bias statistics. As discussed earlier, the bias values may be more related to the method of comparing the model and observations, rather than due to the actual skill of the model. So it is sensible to place most weight here on the SI values.

## 5.2. Evaluation against altimeter data

Even though the altimeter data are directly used in the DA, they can still be used for verifying the forecasts, as they are independent of the model forecast. In this section, the two altimeter data streams are combined and treated as one data source. This provides good spatial coverage over the oceans during the one month period considered here. Statistics are calculated within  $10^\circ$  by  $10^\circ$  boxes at  $5^\circ$  intervals over the globe. Raw data produced by satellites often contain errors, and must be adequately quality controlled before use. During DA, the method of Young and Glowacki (1996) is used, consisting of an initial check for gross error against the first guess field, followed by a cross validation check for consistency with other nearby data. This serves to remove erroneous data, with the comparison with the first guess field also limiting shocks to the model. For the validation data stream, cross validation only is used, maintaining complete independence from the model.

Model data is then bilinearly interpolated in space to the altimeter observation location, and linearly interpolated in time to make up a set of co-locations. For each  $10^\circ$  by  $10^\circ$  box, co-locations are then accumulated for the month period, and statistics evaluated from these co-

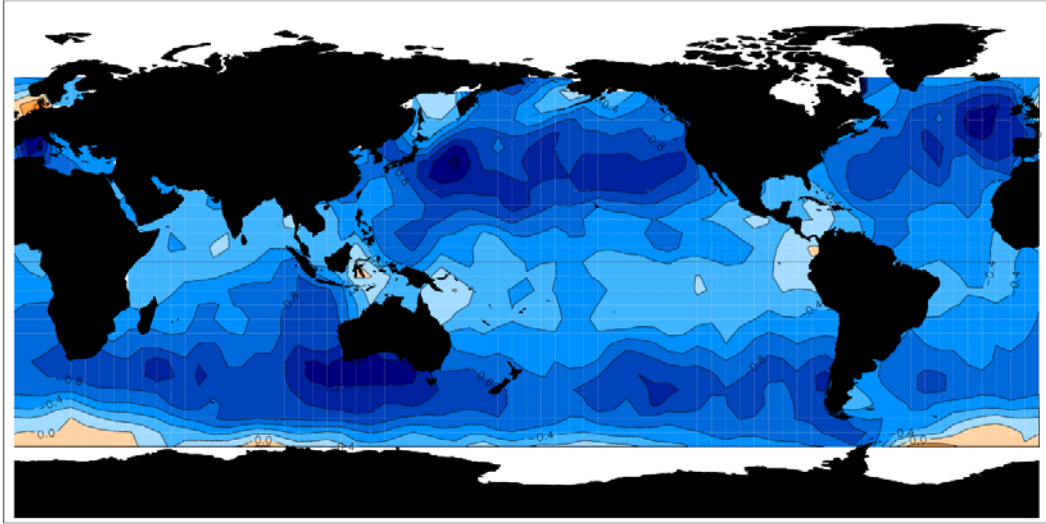


**Figure 11** Bias (Modelled  $H_s$  - altimeter  $H_s$ ) for 24-hour forecasts from the Noassim-12 model run.

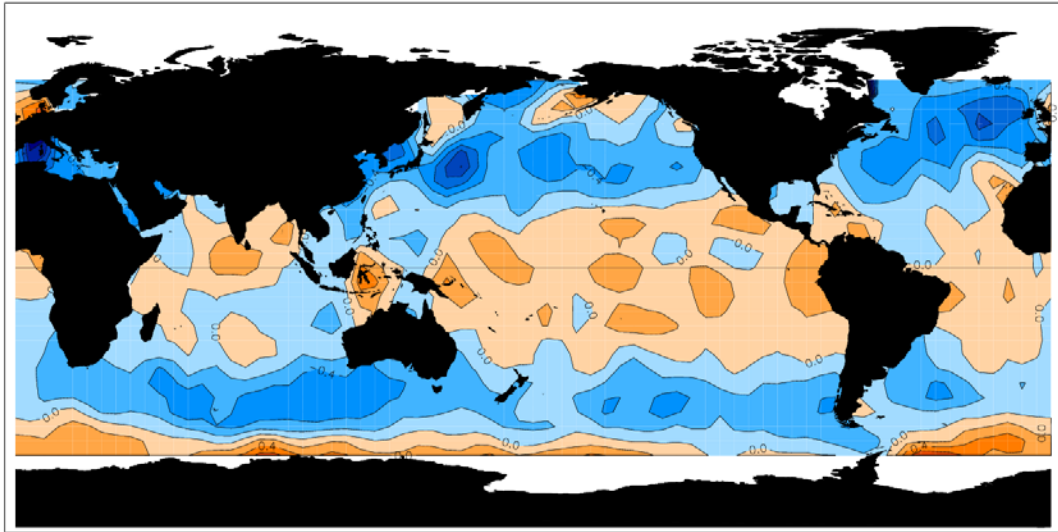


**Figure 12** Same as Figure 11 except for the Both-12 model run.

locations. Figure 11 shows the mean bias over the month for the 24-hour forecasts from the Noassim-12 run.

Not surprisingly, it can be seen the the model is biased low over almost the entire domain. The bias is not evenly distributed though, and reaches more than 1 m in some areas. In general, the largest negative biases exist in mid-to-high latitudes, where the  $H_s$  is highest.

The DA would be expected to remove a large part of this bias. This can be seen in Figure 12,

which shows the bias for the run with twelve directional bins and both satellite data streams assimilated. Most of the areas of high negative bias have disappeared and there are some areas, mainly in the tropics, where in fact the model is biased high.

It is worth noting here the values of the bias around the Australian coast and particularly the West Australian coast. The buoy verifications shown in Figure 10 suggested that the model was biased high relative to the buoys in this region. However, this does not show up in this

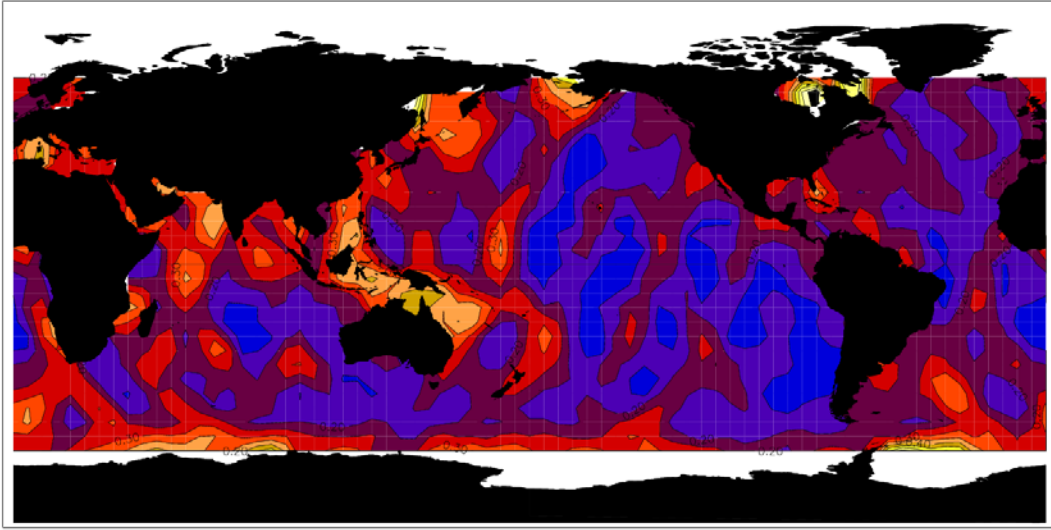


**Figure 13** Scatter Index for 24-hour forecasts from the Both-24 model run.

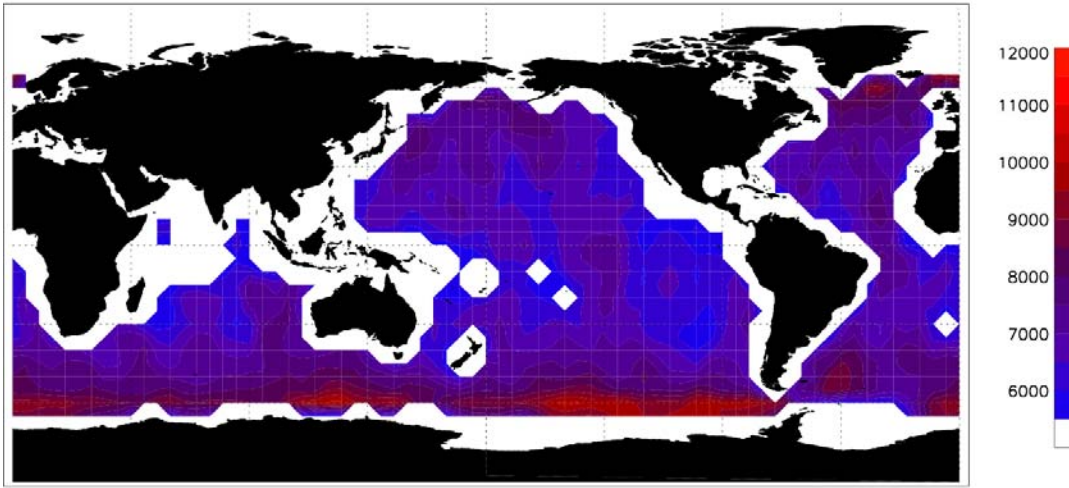


**Figure 14** Number of model/altimeter co-locations in each  $10^\circ$  by  $10^\circ$  box. Only values above 5,500 are plotted.

plot of the spatial distribution of the model bias. This suggests that the positive bias seen at the buoy locations in Figure 10 is a coastal effect, or an artifact of the co-location technique used.

Figure 13 shows the spatial distribution of the SI from the Both-24 model run, as compared to the satellite data. Recall that SI is the square root of the variance of the difference between the observed  $H_s$  and the model  $H_s$  normalised by the mean observed  $H_s$ . It is important to note here that while we have been assuming that the altimeter data are unbiased (this is a reasonable

assumption based on the results of Section 4) we can not similarly assume that the altimeter observations have no variable errors. The variance upon which the SI here is based is therefore the sum of the model error variance and the altimeter error variance. The aim of this section is to compare the error characteristics of different model runs and since the altimeter error variance will not change between each run, we can still use these results for comparison purposes.

A related issue is the issue of scales of

variability. The altimeter data includes variability on considerably smaller spatial scales than the model fields, and the error variances calculated here will include this difference in variability. Ideally, the altimeter observations should be smoothed or averaged so that they represent the same scales as the model. Again, this effect will be same for all model runs, so this is not done for these preliminary assessments, but is left for further work.

It can be seen from Figure 13 that the SI for this run is fairly variable over the globe and ranges from  $\sim 0.15$  to  $\sim 0.35$ . There appear to be patterns of low and high SI that are possibly aligned with the satellite ground tracks. The question arises as to whether this is a result of the irregularly spaced satellite data. Figure 14 shows the number of individual model/altimeter co-locations in each  $10^\circ$  box (above a minimum value of 5,500). The main feature seen here is the higher density of observations at high latitudes – the patterns seen in Figure 13 do not show up here.

Overall statistics for all model runs are shown in Figure 15. Rather than calculating these statistics simply from the set of all altimeter/model co-locations, they are calculated by averaging together the statistics calculated from each  $10^\circ$  by  $10^\circ$  box. While it could be argued that this is not statistically the most robust method, this approach was taken here in the interests of gaining the best overall global picture. Simply using the entire set of co-locations to calculate the statistics would give a higher weighting to the high latitudes where the density of observations is greatest due to the convergence of the altimeter tracks (see Figure 14). In addition, the statistics for each box (i.e. the bias, RMS etc.) are normalised according to latitude. This avoids giving too much emphasis on the statistics of  $10^\circ$  boxes at higher latitudes, which are considerably smaller than  $10^\circ$  boxes at the equator.

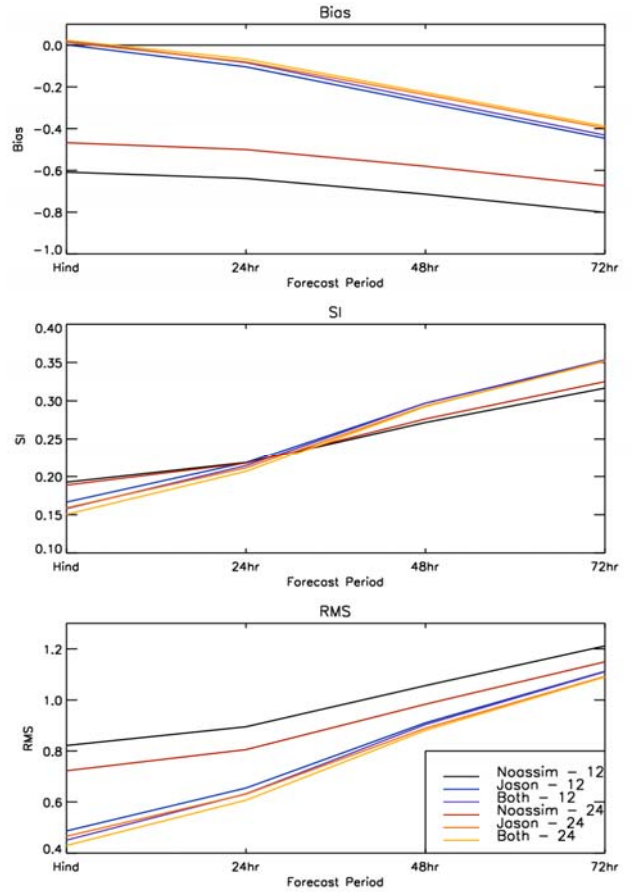


**Figure 15** Summary of verification statistics (Bias, Scatter Index and RMS difference) for all model runs compared to Jason-1 and Envisat satellite altimeter observations.

Some of the features of these verifications are similar to those of the buoy verifications, while there are also some major differences. Consider first the bias statistics. As for the buoy verifications, increasing the directional resolution improves the bias over all forecast periods. Inspection of the spatial distribution of the bias, shows that the increase in directional resolution reduces the bias consistently over the globe. This is possibly due the fact that increasing the directional resolution of the wave spectrum reduces the sprinkler effect and allows propagation of wave energy to a greater number of model grid points. This will therefore result in an increase in the overall  $H_s$ . Another explanation could be that the change in directional resolution changes the amount of shadowing due to islands. Whatever the reason, these results demonstrate that increasing the

directional resolution of the wave spectrum has more of an impact than simply improving the aesthetics of the modelled wave fields, as suggested in WISE Group (2007). This discrepancy could be because here, we are considering a change in directional resolution from  $30^\circ$  to  $15^\circ$ , rather than from  $15^\circ$  to higher resolution. In addition, the sprinkler effect is more pronounced in AUSWAM due to the higher-order propagation numerics. Clarification of these results deserves further investigation.

Note that all the DA runs have a bias that is very close to zero for the hindcasts. This is mainly a reflection of the fact that the hindcasts are not actually independent of the observations that they are being compared to. However, it is worth emphasizing (see Figure 12, for example) that zero bias overall does not mean that the bias is zero everywhere, and in fact the model bias does vary substantially over the globe.

Some aspects of the SI results in Figure 15 are non-intuitive. At the short-range forecasts (less than 24 hours) the results are as expected – the DA cases reduce the variable errors in the model fields, and the assimilation cases with both altimeters perform better than the cases where only Jason-1 is assimilated. However, for the longer range forecasts, it can be seen that the SI is worse for the DA cases than the non-DA cases and in addition, the increase in directional resolution appears to have degraded the modelled  $H_s$  even when DA is not incorporated. This is the opposite to what was seen with the buoy verifications. There is the possibility that the issues discussed earlier in this section relating to the error variances are having an impact on the results seen here. This is also an area that needs further investigation. For this reason, we place less weight on the SI and RMS error values here and more weight on the bias.

### 5.3. Computational usage

Table 3 shows a summary of the computational usage on the NEC SX6 for each model run. The

User time is the average number of CPU seconds for a 12-hour hindcast period and a 72-hour forecast period. Note that all timings are based on running the model on a single processor - these may be different for multi-processor computation.

**Table 3** Computational usage summary for each model run. Jason-12 is highlighted as the current operational configuration.

Run	User time (sec)	Memory size (MB)
Noassim-12	430	1296
Noassim-24	838	2512
<i>Jason-12</i>	<i>664</i>	<i>1312</i>
Jason-24	1070	2528
Both-12	1110	1312
Both-24	1324	2528

The assimilation of Jason-1 data increases the time taken by around 50%. In other words, for a 12-hour hindcast and 72-hour forecast the assimilation of Jason-1 data takes up around one third of the total time. When Envisat is included as well, the time increases substantially and the DA is almost two thirds of the total time.

The increase in the spectral resolution from 12 to 24 directional bins doubles the memory size required, not surprisingly. This also doubles the time taken for the run without DA. For the DA runs, the increase in time due to the increase in directional resolution applies only to the non-DA component of the total time, so the impact is not so large. For Jason-1 alone, the increased spectral resolution increases the time by 60% and if data from both satellites is assimilated, the increase in resolution increases the time by only 20%.

### 5.4. Preliminary Conclusions

The verification of the various model runs against buoys in the Australian region

suggested that improvements in the variable errors at short forecast ranges would come mainly from including both satellite data streams in the DA, while improvements in skill for longer forecast ranges would come mainly from increasing the directional resolution. The verification against the altimeter data suggested that if the directional resolution is doubled, then including Envisat data in the DA as well, will produce only a marginal improvement in the bias. However, a consideration of the computational requirements of both of these enhancements showed that the resources required to enhance the current system either by increasing the directional resolution or by including more altimeter data are almost equivalent. Further to this, if one of these upgrades is implemented, then they may as well both be implemented as the computational requirements to implement both are not that much greater than the requirements for implementing only one.

## 6. Summary and Further Work

Fast delivery  $H_s$  data from both the Jason-1 and Envisat altimeters have been validated against in situ buoy data. Jason-1 is found to be performing consistently throughout the range of wave heights and requires no correction. Consistent with previous work, it is found to be rather noisy, certainly more so than Envisat. The RMS difference between Jason-1 and buoy data is 0.229 m. Envisat is overestimating low  $H_s$  and underestimates high. A linear correction reduces the RMS from 0.219 m to 0.202 m, an 8% reduction. This lower corrected RMS relative to Jason-1 is a reflection of the noise in the Jason-1 data.

A systematic difference in the  $H_s$  being reported by MEDS and NDBC buoy networks is noted. Using the altimeter data as a common reference, it is estimated that MEDS buoys are underestimating  $H_s$  relative to NDBC buoys by about 10%.

The corrected altimeter data were used to make preliminary assessments of two potential upgrades to the Bureau's wave forecasting

system – specifically, an increase in the directional resolution of the wave spectrum and the expansion of the data assimilation system to include Envisat  $H_s$  data as well as Jason-1. *In situ* buoy data were also used to assess the improvements in model forecast skill and the computational requirements of the potential upgrades were evaluated.

Various issues associated with the verification techniques were discussed, such as the proximity of the buoys to the Australian coast, and the error variance of the altimeter observations. Based on these issues, it was suggested that preliminary conclusions should be made based on the SI values from the buoy verifications and the bias values from the altimeter verifications. The conclusions from the buoy verifications were that for short ranges, the best results would be obtained from assimilating both sets of altimeter data, while for longer range forecasts, the best results are obtained from the increased directional resolution.

Assessment of the bias between the model  $H_s$  and the altimeter data showed that the increase in the directional resolution has a positive impact on the bias in the non-assimilated model fields. It was also found that there was very little difference between all the DA cases at short forecast ranges. In addition, it was shown that the bias varies significantly over the globe.

The results shown here are preliminary evaluations of modelled wave fields. There are numerous aspects to this work that requires further development. In particular, there are several aspects to the way in which the comparisons between modelled, buoy and altimeter  $H_s$  have been performed that could be improved. For example, the gridded model fields could be interpolated in space to the buoy locations and the buoy observations should be smoothed so that they represent the same scales of variability as the model. Similarly, the altimeter observations should be processed in order to remove the variability on short spatial scales.

These initial verifications have provided some interesting results that deserve further investigation. For example, there is a ubiquitous decrease in the negative bias that occurs when the directional resolution is increased. It would be interesting to assess to what extent this occurs for different spatial model resolutions.

This study has only considered a global implementation of AUSWAM. The current operational implementation at the Bureau incorporates a higher resolution regional model nested within the global model and a further higher resolution model nested within the regional model. There has been an inherent assumption that if the global model skill is improved, this will also feed into better regional model forecasts. This would occur because a) the enhancements made on the global scale are assumed to also be effective at the regional scale and b) an improved global model provides higher quality boundary conditions for the nested models. This needs to be confirmed by considering a nested regional model incorporating the proposed enhancements and comparing the resulting modelled wave fields against altimeter data in the Australian high seas regions.

The spatial distribution of the bias seen in these results is likely to be due to either errors in the winds used to force the wave model, or deficiencies in the wave model physics. Satellite scatterometers provide an ideal source of marine wind observations and once the characteristics of the wind forcing errors are known, then the wave model physics can be considered more closely. This is planned for further work, and will be especially relevant in the context of a new atmospheric model that is planned for operational implementation at the Bureau in the near future.

## Acknowledgements

The authors would like to thank a number of people for contributions to this work. Jean-Michel Lefevre (Meteo-France), and the European Space Agency for providing some Jason-1 and Envisat data respectively and

Graham Warren and Mikhail Entel for help retrieving archived data at the Bureau. Comments made on the manuscript by Eric Schulz and Jeff Kepert are also greatly appreciated.

## References

- Abdalla, S., 2006: Global Validation of ENVISAT Wind, Wave and Water Vapour Products from RA-2, MWR, ASA and MERIS. *ESA Contract Report 17585*.
- Abdalla, S., J. Bidlot, and P. Janssen, 2005: Jason Altimeter Wave Height Verification and Assimilation. 2005: Jason Altimeter Wave Height Verification and Assimilation, In: Ozhan, E. (Editor), *Proceedings of the Seventh International Conference on the Mediterranean Coastal Environment (MEDCOAST 05)*, Kusadası, Turkey, 25-29 Oct. 2005, 1179–1185.
- Bauer, E., and C. Staabs, 1998: Statistical properties of global significant wave heights and their use for validation. *J. Geophys. Res.*, **103**, 1153–1166.
- Bidlot, J., P. Queffeulou, T. Durrant, and D. J. M. Greenslade, in prep: Discrepancies in wave height measurements between observing networks. Technical report, ECMWF.
- Caires, S., and A. Sterl, 2003: Validation of ocean wind and wave data using triple collocation., *J. Geophys. Res.*, **108**, 3098.
- Caires, S., A. Sterl, J. R. Bidlot, N. Graham, and V. Swail, 2004: Intercomparison of different wind-wave reanalyses. *J. Clim.*, **17**, 1893–1913.
- Carayon, G., N. Steunou, J. Courrière, and P. Thibaut, 2003: Poseidon-2 Radar Altimeter Design and Results of In-Flight Performances. *Marine Geodesy*, **26**, 159–165.
- Challenor, P. G., and P. D. Cotton, 2001: The joint calibration of altimeter and in situ wave heights. *Advances in the Applications of Marine Climatology - The Dynamic Part of the WMO Guide to the Applications of Marine Climatology*, WMO Geneva, volume WMO/TD-No. 1081.
- Cotton, P., D. Carter, P. Challenor, and V. Kareev, 2001: A coordinated programme for global calibration/validation of altimeter sea state data. AVISO.
- Cotton, P., P. G. Challenor, and J.-M. Lefevre, 2004: Calibration of ENVISAT and ERS-2 wind and wave data through comparison with in-situ data and wave emodel analysis fields. ENVISAT

- ERS Symposium, ESA SP572, Salzburg, Austria.
- Cotton, P. D., and D. J. T. Carter, 1994: Cross calibration of topex, ERS-1, and GEOSAT wave heights. *J. Geophys. Res.*, **99**, 25025–25033.
- Desai, S. D., and P. Vincent, 2003: Statistical Evaluation of the Jason-1 Operational Sensor Data Record. *Marine Geodesy*, **26**, 187–199.
- Durrant, T., Greenslade, D.J.M. and I. Simmonds, Validation of Jason-1 and Envisat Remotely Sensed Wave Heights, *submitted to J. Atmos. Oc. Tech.*
- Greenslade, D., and I. Young, 2004: A validation of ERS-2 Fast Delivery Significant Wave Height. *BMRC Research Report No. 97*, Bureau of Meteorology Research Centre.
- Greenslade, D.J.M. and I.R. Young, 2005: The impact of inhomogenous background errors on a global wave data assimilation system, *J. Atmos. Oc. Sci.*, **10**, No. 2 doi:10.1080/17417530500089666.
- Greenslade, D.J.M., E. W. Schulz, J. D. Kepert and G.R. Warren, 2005: The Impact of the Assimilation of Scatterometer Winds on Surface Wind and Wave Forecasts, *J. Atmos. Oc. Sci.*, **10**, No 3, doi:10.1080/17417530600784976
- Faugere, Y., J. Dorandeu, F. Lefevre, N. Picot, and P. Femenias, 2006: Envisat ocean altimetry performance assessment and cross-calibration. *Sensors*, **6**, 100–130.
- Janssen, P. A. E. M., B. Hansen, and J. R. Bidlot, 1997: Verification of the ECMWF wave forecasting system against buoy and altimeter data. *Weather and Forecasting*, **12**, 763–784.
- Ménard, Y., L. Fu, P. Escudier, F. Parisot, J. Perbos, P. Vincent, S. Desai, B. Haines, and G. Kunstmann, 2003: The Jason-1 Mission. *Marine Geodesy*, **26**, 131–146.
- Monaldo, F., 1988: Expected differences between buoy and radar altimeter estimates of wind-speed and significant wave height and their implications on buoy altimeter comparisons. *J. Geophys. Res.*, **93**, 2285–2302.
- National Meteorological and Oceanographic Centre, 2002: Changes to the Operational Sea State Forecast System, *Analysis and Prediction Operations Bulletin No. 55*, Bur. of Meteorology.
- Queffeuilou, P., 2004: Long-Term Validation of Wave Height Measurements from Altimeters. *Marine Geodesy*, **27**, 495–510.
- 2006: Altimeter wave height validation: an update. *Ocean Surface Topography Science Team 2006 meeting*, Venice, 16-18 March.
- Ray, R., and B. Beckley, 2003: Simultaneous Ocean Wave Measurements by the Jason and Topex Satellites, with Buoy and Model Comparisons. *Marine Geodesy*, **26**, 367–382.
- Resti, A., J. Benveniste, M. Roca, G. Levrini, and J. Johannessen, 1999: The Envisat Radar Altimeter System(RA-2). *ESA Bulletin*, **98**, 94–101.
- Schulz, E. W., J. D. Kepert, and D. J. M. Greenslade, 2007: An Assessment of Marine Surface Winds from the Australian Bureau of Meteorology Numerical Weather Prediction Systems, *Wea. and Forecasting*, **22**, No. 3, pp 609 - 632.
- Soukissian, T., and C. Kechris, 2007: About applying linear structural method on ocean data: Adjustment of satellite wave data. *Ocean Engineering*, **34**, 371–389.
- Tolman, H L., 2002a: Alleviating the Garden Sprinkler Effect in wind wave models, *Ocean Modelling*, **4**. pp 269 – 289.
- Tolman, H. L., 2002b: Validation of WAVEWATCH III version 1.15 for a global domain. Technical Note Nr. 213 p 33, NCEP.
- WAMDI Group (S. Hasselmann, K. Hasselmann, E. Bauer, P.A.E.M. Janssen, G. Komen, L. Bertotti, P. Lionello, A. Guillaume, V.C. Cardone, J.A. Green-wood, M. Reistad, L. Zambresky, and J.A. Ewing), 1988: The WAM model - A third generation ocean wave prediction model. *J. Phys. Oceanogr.*, **18**, 1775-1810.
- WISE Group (Cavaleri L., J.-H. Alves, F. Ardhuin, A. Babanin, M. Banner, K. Belibassakis, M. Benoit, M. Donelan, J. Groeneweg, T.H.C. Herbers, P. Hwang, P.A.E.M. Janssen, T. Janssen, I.V. Lavrenov, R. Magne, J. Monbaliu, M. Onorato, V. Polnikov, D. Resio, W.E. Rogers, A. Sheremet, J. McKee Smith, H.L. Tolman, G.van Vledder, J. Wolf, I. Young), 2007: Wave modelling – the state of the art, *Progress in Oceanography*, in press.
- Young, I. R., and T. J. Glowacki, 1996: Assimilation of altimeter wave height data into a spectral wave model using statistical interpolation, *Ocean Eng.*, **23**(8), 667–689.